Acta Geochim (2019) 38(6):883–896
https://doi.org/10.1007/s11631-019-00375-5

ORIGINAL ARTICLE

Petrogenesis, geochemistry and geological significance of Paleocene Granite in South Gangdese, Tibet

Chengzhi Li[1] · Wenguang Yang[2] · Lidong Zhu[2] · Zhen Yang[3] · Limin Lin[2] · Xin Su[2] · Hongliang Zhang[1]

Received: 7 March 2019 / Revised: 12 July 2019 / Accepted: 3 September 2019 / Published online: 10 September 2019

Abstract The Gangdese magmatic belt, located along the southern margin of the Lhasa terrane, plays a critical role in understanding the tectonic framework associated with the Indian–Asian slab collision. In this paper, a chronology of zircon U–Pb and geochemical analysis of the rock of the Cuobulaguo granitic mass in the southern of the Gangdese, Tibet, revealed a series of results. The results show that the LA-ICP-MS monzonitic granite zircon U–Pb ages are 61–59 Ma, which corresponds to the same period as the magmatic arc of the southern limit of Gangdese. In terms of geochemical composition, the granite is rich in $\omega(SiO_2)$ 70.09% to 72.64%, with a high $\omega(Al_2O_3)$ 14.40% to 15.99%, a low $\omega(TiO_2)$ 0.08% to 0.24%, $\omega(MgO)$ 0.41% to 0.76%, $\omega(Fe_2O_3^T)$ 6.82% to 29.9%, $\omega(P_2O_5)$ 0.07% to 0.12%, and $\omega(CaO)$ 1.06% to 1.75%. The granite mainly belongs to the high-K calc-alkaline series. The light rare earth element (LREE) content of skeletal granite is between $133.69 \times 10^{-6} \sim 226.64 \times 10^{-6}$ and the heavy rare earth element (HREE) content is between 17.36×10^{-6} and 32.11×10^{-6}. LREE/HREE is between 5.05 and 7.83. It is enriched in light rare earth elements (LREE) and large ion lithophile elements, such as Rb, K, U, etc., depletes high field strength elements, such as P, Nb, and Ta, and has the geochemical composition of arc magmatic rocks. In addition, the aluminum saturation index (A/CNK = 1.06 to 1.11) of Cuobulaguo granite, belongs to I-type granite. The comprehensive analysis showed that with the beginning of the collision between the Indian–Asian continental, the subduction ocean plate was separated from the continental plate due to gravity, resulting in an increase in the asthenosphere, which made partial fusion of the lithospheric mantle. It invaded the bottom of the lower crust, which in turn induced a partial melting of the lower crust to form granite.

Keywords Petrogenesis · Zircon U–Pb dating · Cuobulaguo granite · South margin of Gangdese · Tibet

1 Introduction

The Qinghai-Tibet Plateau is known as the "roof of the world" and is an ideal place to study the dynamics of the continent (Yin and Harrison 2000; Mo et al. 2009a; Xu et al. 2011; Zhang et al. 2017). The Lhasa Terrane contains essential information, as well as more collisions and orogenic evolution of the Neo-Tethys oceanic (Mo et al. 2003, 2007). Acidic volcanic rocks in southern Gangdese are typical, which provide a collisional evolution of the Indian–Asia continent, and subduction to the north of the New-Tethys slab provide evidence (Chung et al. 2003, 2005, 2009; Dong et al. 2008; Chu et al. 2006, 2011; Mo et al. 2005, 2009a, b; Pan et al. 2006; Hou et al. 2008; Ji et al. 2009a, b; Xu 2010; Ma et al. 2017; Zhu et al. 2008, 2011, 2015, 2017; Zhang et al. 2013a, b, 2017; Tang et al. 2015; Wang et al. 2015; Sun et al. 2017). However, both the nature of the Early Eocene magmatic rocks within

Electronic supplementary material The online version of this article (https://doi.org/10.1007/s11631-019-00375-5) contains supplementary material, which is available to authorized users.

✉ Wenguang Yang
yangwg1018@gmail.com

[1] School of Earth Sciences, Chengdu University of Technology, Chengdu 610059, China

[2] Institute of Sedimentary Geology, Chengdu University of Technology, Chengdu 610059, China

[3] No. 282 Brigade, Sichuan Bureau of Geology for Nuclear Industry, Deyang 618000, Sichuang, China

the belt and their tectonic history are still debated. Early work believed that the Palcoccne granitoids were caused by the subduction of the Neo-Tethys oceanic slab (Searle et al. 1987; Xu et al. 2011; Ji et al. 2016). More recent work systematically studied the Linzizong volcanic rocks and, through this system, thought that the collision caused the subduction of the Neo-Tethyan oceanic slab roll-back and break-off (Mo et al. 2003, 2005, 2008; Xu 2010). In recent years, a large number of scholars have carried out research on the magma evolution of the Gangdese rock foundation. The magmatic rock belt of Gangdese is a complex rocky base formed by multistage magmatism. The granite in this region consists mainly of magmatic arc-shaped rocks, which show the characteristics of the mantle with losses or the area of the main source of the crust (Chung et al. 2003). In addition, many scholars have discussed the timing of the collision between the Indian–Asia continent and the geochemical characteristics of the magmatic rocks. Most researchers believe that the collision time of the Indian–Asia continent is the Early Eocene ($\sim$ 55 Ma) (Ji et al. 2009a, 2016; Xu et al. 2011; Donaldson et al. 2013; Zhu et al. 2015; Hu et al. 2015, 2016). However, some scholars believe that this event occurred at approximately 45 Ma (Wang 2017). In addition, the genesis of the magmatic activity in the southern belt of Gangdese is usually due to subduction in the by Neo-Tethys oceanic and the magma that underlies the collision between Indian and Asia continent. The "break-off" and "roll-back" of the Neo-Tethys oceanic slab are considered the general overview of deep magmatism in the southern Gangdese belt (Wen et al. 2008a, b; Ji et al. 2012, 2016; Wang 2016; Wang et al. 2015; Zhu et al. 2015; Ma et al. 2017).

In this study, we present zircon U–Pb ages of granite rock from the Cuobulaguo in the southern margin of the Lhasa country. Then, we analyzed petrogenesis, source of magma and the geodynamic configuration of granite. The new information is beneficial to our understanding of the genesis and formation of magma in the southern Gangdese belt and also provides new information about the collision process of the Indian–Asia continent.

2 Geological background

Qinghai-Tibet Plateau, respectively, from north to south to Jinsha Suture Zone (JSSZ), Bangong-Nujiang Suture Zone (BNSN) and Yarlung-Tsangpo Suture Zone (YZSN) for the delineation of Songfan-Ganzi Terrane, Qiangtang Terrane, Lhasa Terrane, and Himalayan Terrane (Fig. 1a). The Lhasa Terrane is also known as the "Gangdese Terrane" (Mo et al. 2005; Pan et al. 2006; Zhu et al. 2008), with an east–west longitude of about 2500 km and a north–south width of about 100 to 300 km. The Gangdese terrane can be divided into the northern, central, and southern subterranes, bounded by the Shiquanhe-Nam Tso Mélange Zone (SNMZ) and Luobadul-Milashan Fault (LMF) (Zhu et al. 2006, 2008) (Fig. 1b). The north of Gangdese and the south of Gangdese are characterized by juvenile crust. Central Gangdese is mainly characterized by ancient crust (Pan et al. 2006; Zhu et al. 2008, 2011, 2015). In the central subterrane of Gangdese Terrane, Carboniferous-Permian meta-sedimentary sequences and Lower Cretaceous volcano-sedimentary sequences are intruded by widespread Mesozoic granite ($\sim$ 210–90 Ma) (Allègre and Rousseau 1984; Zhu et al. 2011), Paleocene-Eocene granite (Ji et al. 2009a, b, c), and volcanic rocks of the Linzizong Volcanic Succession (Mo et al. 2007). This new study focuses on the southern subterrane of Gangdese (Fig. 1b). This basement has undergone the subduction of the Neo-Tethys oceanic slab and the India-Asia continental collision (Yin and Harrison 2000; Mo et al. 2005; Chu et al. 2006) However, in the eastern part of Gangdese southern subterrane, Early Paleozoic granites were discovered (Dong et al. 2005), suggesting that the old crystalline basement may be present locally in this subterrane. South of the Gangdese, the Cretaceous magmatic rocks of the Lower Mesozoic develop mainly at the base of Cretaceous rocks -negénico of Gangdese and in the volcanic rocks of the Linzizong Paleógeno. Recent research indicates, the magmatism was generated mainly between the Upper Cretaceous and the Paleogene after the collision between an Indian–Asian continent and subduction to the north of the Neo-Tethys oceanic slab due to the severity.

The granitic region of Cuobulaguo is located on the southern Gangdese terrane. The rock mass was produced in an irregular rock mass from east to west with an exposed area of about 60 km^2 (Fig. 1c). The rock mass is divided into marginal phase and central phase. The intrusive strata are mainly the Yeba ($J_{2-3}y$) and Chumulong (K_1c) formations. The contact zone often has a contact metamorphism, such as silicification, horn lithification, and skarnisation phenomenon. The brown mass of the fault is better in the field (Fig. 2a). The main rock types are medium-fine-grained monzonitic granites with a massive structure and a fine-grained granitic structure (Fig. 2b, c). The main minerals include quartz (28% to 30%), K-feldspars (30% to 38%), plagioclase (25% to 30%), and biotite (5% to 10%) and hornblende (less than 2%), apatite minerals, metals and other minerals with particle sizes between 2 and 6 mm (Fig. 2d, e). Quartz has a granular shape and is distributed unevenly. It is often replaced by alkali feldspar and plagioclase. Plagioclase is a semi-formed self-formed plate, with many double crystals or polycrystalline channels, and its surface is sometimes altered by chlorite. The K-feldspars have a semi-automatic shape, a plate shape and two transparent crystals in the form of a card. It is composed

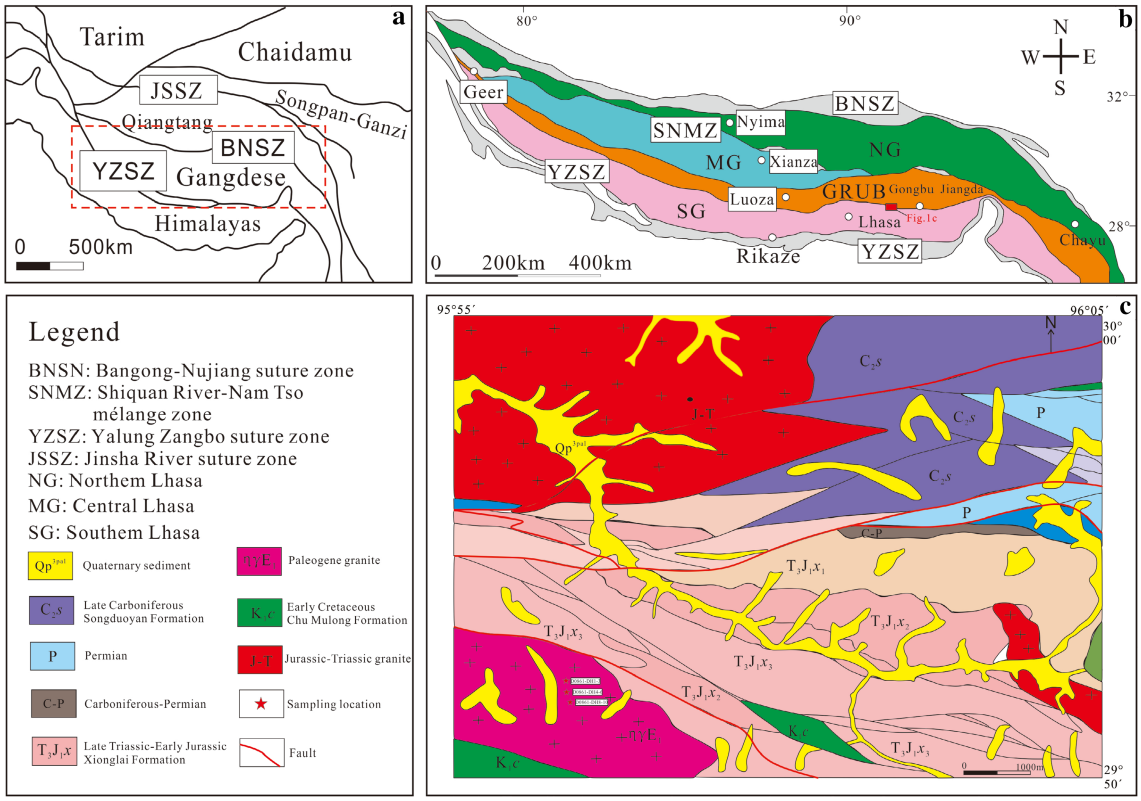

Fig. 1 The geological map of the Tibet Plateau (**a**) and the Gangdese tectonic unit (**b**) (according to Zhu et al. 2009) and the geological distribution of the Cuobulaguo granite (**c**)

mainly of striped feldspar and feldspar, and its particle size is 0.2 to 6 mm. A small amount of quartz is replaced by potassium feldspar, which contains a structure and a slight alteration of the clay. The biotite is brown and scaly, with a small amount of meteorite and chlorite alteration, distributed between plagioclase, alkali feldspar and quartz particles, and has a low green mud and petrochemical.

3 Analytical methods

The zircon samples were separated and selected in Langfang City, Hebei Province, Yuheng Rock Mine Technology Services Co., Ltd., after the sample was milled and washed, the standard technology of separation of heavy liquids and Magnetic was used to extract the zircon. Samples of zircon and cathodoluminescence photomicrography were completed at Beijing Zirconium Leading Technology Co., Ltd., and the zircon particles without glass or cracks were selected under a binocular microscope, and the zircon was applied on the double-sided tape. It was fixed with epoxy resin and polished until the inside of the grain was exposed. Prior to analysis, the surface was cleaned with 3% HNO_3 to remove any lead contaminants. The zirconium particles were polished to half the original particle size to obtain zirconium cathode photoluminescence (CL) images. The Zircon U–Pb dating analysis was performed by Wuhan Shangpu Analysis Technology Co., Ltd. using the LA-ICP-MS method. The GeolasPro laser ablation test system used in the experiment included a MicroLas optical system and a COMPexPro 102 ArF laser excimer 193 nm with a laser ablation beam and a frequency of 32 μm and 10 Hz, respectively. In the process of laser ablation, helium was used as the carrier gas for the ablation material, and argon as the compensation gas. The zirconium U–Pb and the trace elements were corrected. By fractionation of isotopes and trace elements according to the zircon standard 91,500 and the glass material standard NIST610 as external standards. Data processing was performed using the ICPMS DataCal software (Liu et al. 2010). The age harmonic map of the U–Pb zircon and the calculated weighted average age were calculated using Isoplot/Ex_ver3 (Ludwig 2003). Relative error 1σ of individual test data, for zircon $^{206}Pb/^{238}U$ Age > 1000 Ma with $^{207}Pb/^{206}Pb$, otherwise with $^{206}Pb/^{238}U$ of age. The results of the test are shown in Supplementary materials Table 1.

The content analysis of major-elements, trace-elements, and rare-earth-elements was completed at the Laboratory of Isotope Geochemistry, Guangzhou Institute of Geochemistry. The analysis accuracy of the main elements was

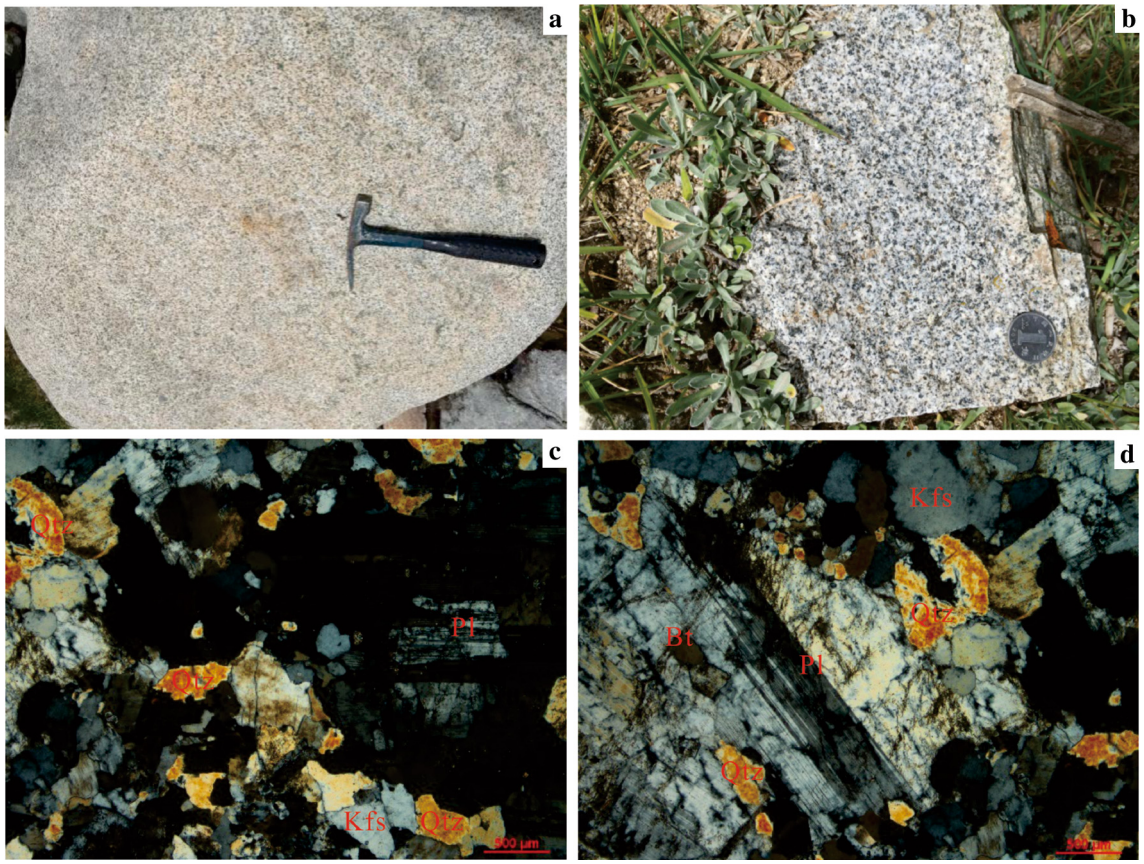

Fig. 2 Cuobulaguo granite outcrop (**a**, **b**) and microscopic photos (**c**, **d**) Qtz, quartz; Pl, plagioclase; Kfs, potassium feldspar; Bt, biotite

better than 2%. The glass cake was made by alkali fusion method and analyzed by Rigaku 100e X-ray fluorescence spectrometer (XRF); Trace elements using Perkin-Elmer Elan 6000 inductively coupled plasma mass spectrometer (ICP-MS) analysis, the accuracy of trace elements in the sample is less than 10×10^{-6} better than 10%, the content is more than 10×10^{-6} analysis accuracy of better than 5%;The rare earth element analysis accuracy of the sample is better than 5%. The detailed analysis process and related parameters can be seen (Liu and Liu 1996), and the test results are shown in Supplementary materials Table 2.

4 Analysis results

4.1 Zircon U–Pb geochronology

The zircon separated from the Cuobulaguo granite were analyzed to obtain precise geological ages. CL images of zircon grains are shown in Fig. 3. The white circles represent the domains of U–Pb citations. The zircon particles in the sample (D0861-N1) are mainly eduèdric and have long to short prismatic shapes with average crystalline lengths of 65–170 μm and a length to width ratio of up to 2:1 or 3:1. Most zircons in CL images were transparent and colorless to slightly brown, with oscillatory zoning typical of magmatic growth. Some zircon particles had a nuclear boundary structure; the zircon nucleus was darker in color and the oscillatory zoning was not developed. 25 dating analyzes were performed in 25 zircons, with the exception of one point error and two harmonics less than 90%, and the other 22 zircons had a Th content of 36.8×10^{-6} to 590×10^{-6}, a content of 40.9×10^{-6} to 1715×10^{-6}, Th/U ratios ranging from 0.36 to 2.63, greater than 0.1, indicating a magmatic origin; U–Pb analyses of 22 granitic zircons (D0861-N1) gave a $^{206}Pb/^{238}U$ concordance of 56 ± 6 Ma at 195 ± 3 Ma (Supplementary materials Table 1), most of which were located in or near the harmonic line; Zircon D0861-N1-01 apparently had an advanced age of $^{206}Pb/^{238}U$ of 195 ± 3 Ma, which may be the age at which zircon was captured. The remaining 21 zircons of $^{206}Pb/^{238}U$ are 56 ± 6 to 67 ± 3 Ma, and the weighted mean age was 61.3 ± 1.4 Ma (Fig. 3b). Therefore, the D0861-N1 sample was generated in the Paleocene, which represents the crystalline age of the rock mass.

The zircon particles of the sample (D0862-N1) were mostly euhedral prismatic crystals with a length of

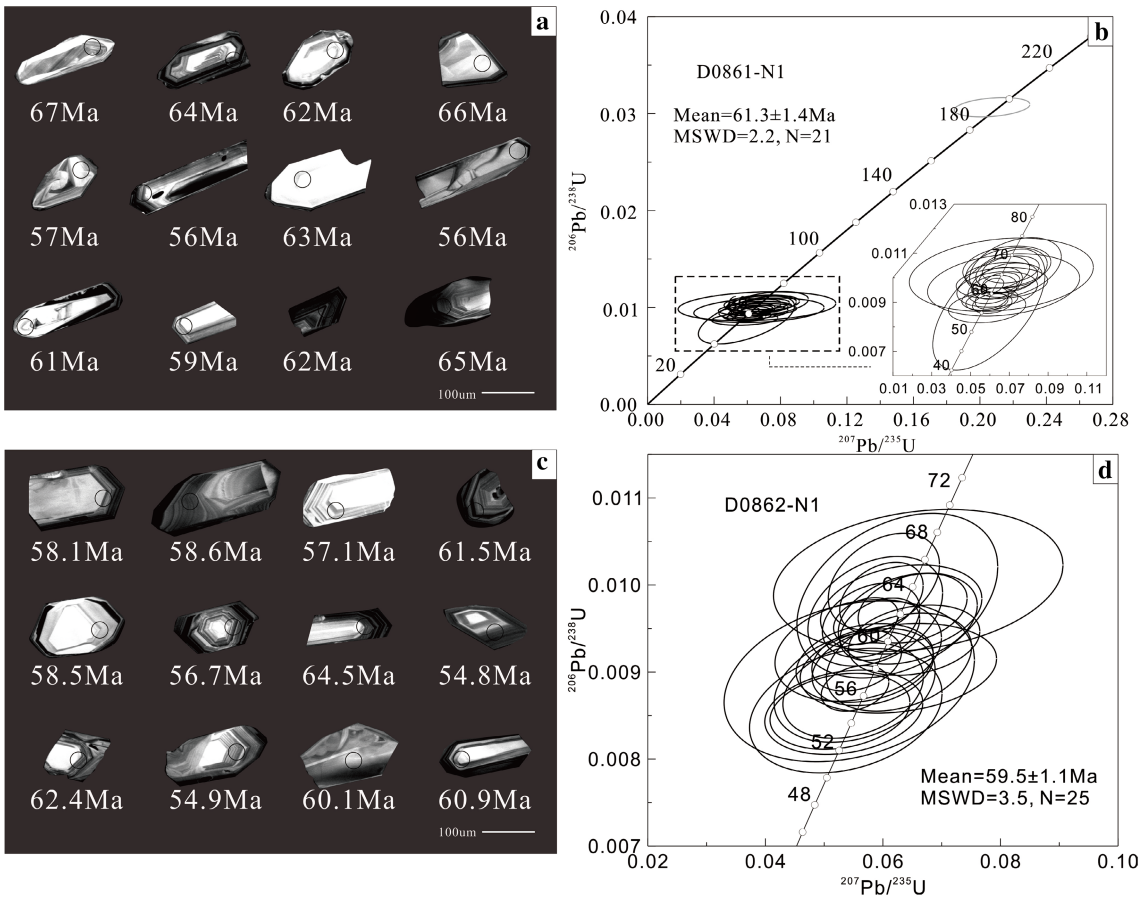

Fig. 3 Zircon cathode luminescence image (**a**, **c**) and U–Pb harmonic age diagram (**b**, **d**)

80–230 μm, a width of 30–110 μm, and length-to-width-ratios of up about 2:1 to 3:1. Most zircons in the CL images were transparent and colorless to slightly brown and display oscillatory zoning typical of magmatic growth. 25 dating analyses were performed on 25 zircons. The zircon Th content of the measured was 45.2×10^{-6} to 481×10^{-6}, U content was 69.4×10^{-6} to 1111×10^{-6}, Th/U ratios ranging from 0.31 to 2.41, indicating a magmatic origin; The 25 zircon U–Pb analyses from sample (D0862-N1) yielded concordant $^{206}Pb/^{238}U$ ages of 54.9 ± 1.1 to 64.5 ± 2.1 Ma with a weighted mean $^{206}Pb/^{238}U$ age of 59.5 ± 1.1 Ma (Fig. 3d). These ages were mostly located on or adjacent to the harmonic line. The Paleocene represents the age of early magmatic diagenesis.

4.2 Whole rock geochemistry

4.2.1 Major elements

The principal component compositions of the granuloid assemblages of the Cuobulaguo pluton are listed in Supplementary materials Table 2. Granitioids have a relatively wide range of SiO_2. The SiO_2 content of the Cuobulaguo pluton varies from 70.09% to 72.64%, which is characterized by a high content of $\omega(Al_2O_3)$ 14.40% to 15.99%, low $\omega(TiO_2)$ 0.08% to 0.24%, $\omega(MgO)$ 0.41% to 0.76%, $\omega(Fe_2O_3^T)$ 6.82% to 29.9%, $\omega(P_2O_5)$ 0.07% to 0.12% and $\omega(CaO)$ 1.06% to 1.75%. On a total alkali and silica TAS diagram, the samples plot mostly in the granite fields and show a sub-alkaline affinity (below dotted line) (Fig. 4), which is fundamentally consistent with the results of the identification of the slice. The DI (differential index) of the sample was 73.28 to 89.35, $Mg^{\#}$ (magnesium index) (6.70 to 13.60). These rocks have Na_2O and K_2O contents of 3.86% to 4.75% and 3.51% to 5.55%, respectively, with $(Na_2O + K_2O)$ from 7.91% to 9.44%, with the K_2O/Na_2O ratios of 0.74 to 1.43 and a value average of 1.05. Moreover, the samples from the granitoid rocks were mainly plotted in the field of the high K Calc-alkaline and shoshonite series on the SiO_2 versus K_2O diagram (Fig. 5a). On the A/NK versus A/CNK diagram (Fig. 5b), most of the samples were weak peraluminous. The similarity is also shown on the Harker diagrams, the samples show good linear relationships between SiO_2 and major oxides (Fig. 6).

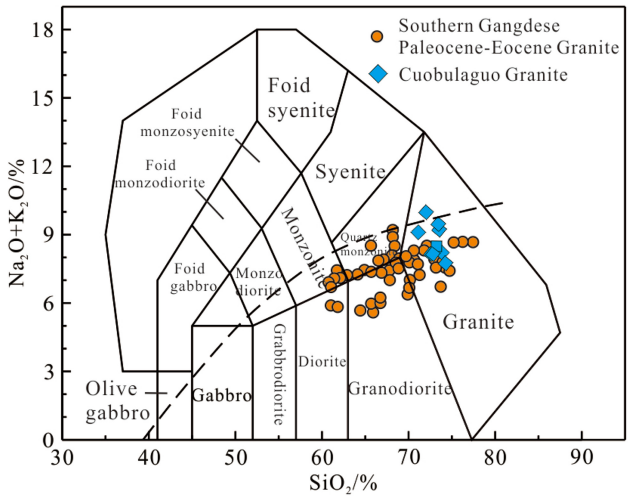

Fig. 4 TAS diagram of the Cuobulaguo granite (according to Middlemost 1994). Other Eocene granite in the southern Gangdese terrane are from Xu (2010)

4.2.2 Rare earths and trace elements

All analytical results are listed in Supplementary materials Table 2. The chondrite-normalized rare earth element patterns suggest that these rocks have similar geochemical characteristics (Fig. 7a). The sample total REE contents of 151.21×10^{-6} to 257.66×10^{-6}, the mean value is 227.75×10^{-6}, slightly higher than the upper crust average total (210×10^{-6}) (He et al. 2005). They are characterized by an enrichment of light rare earth elements (LREEs) and a depletion of heavy rare earth elements (HREEs), LREE/HREE is 5.05–7.83, $(La/Yb)_N$ of 4.48–7.93 and the average value was 6.2. All samples have moderately-strong Eu negative anomalies (δEu of 0.35 to 0.51), showing a very consistent distribution pattern with the upper crust, which is consistent with the presence of plagioclase or potassium feldspar cumulates. The primitive mantle normalized trace elements pattern show that samples are relatively enriched in the large ion lithophile elements (LILEs), such as Rb, Th, and K. Among the high-field-strength elements (HFSE), the samples show negative Nb, P, Ba, Ti anomalies (Fig. 7b). These geochemical features are similar to those of the South Gangdese Eocene granite, such as the Qushui granite masses, Namulin granite masses and Xietongmen granite masses (Xu 2010; Meng et al. 2018).

5 Discussion

5.1 Petrogenesis

The granitoid rocks are divide into A, I, M, and S types based on their geochemical and mineral compositions (Chappell and White 1974; Chappell 1999; Bonin 2007). In general, alkaline melanocratic minerals (e.g., aegirine and riebeckite) are regarded as typical minerals of A-type granite. Superfluous muscovite, sillimanite, and cordierite are associated with S-type granite. The I-type granite was characterized by hornblende and the absence of peraluminous minerals (Whalen and Chappell 1988). The aluminum saturation index A/CNK of the granite in the study area was less than 1.1 and the A/CNK-A/NK low series of over-alumina. The types of aluminous and peraluminous rock were generally considered decompression and fusion heating in the context of shortening of the earth's crust at the beginning of the collision or in the context of rapid rise of the crust and detachment of the crust extension (Zhu

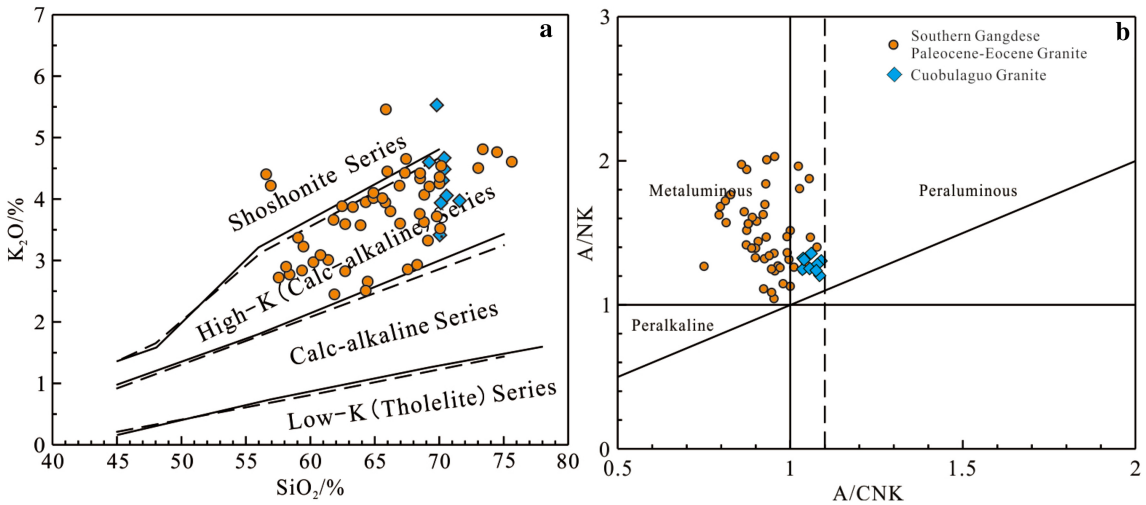

Fig. 5 Chemical classification diagram of the Cuobulaguo granite: K_2O versus Si_2O diagram (**a** according to Rickwood 1989) and A/NK versus A/CNK diagram (**b** according to Peccerillo 1976). Other Eocene granite in the southern Gangdese terrane are from Xu (2010)

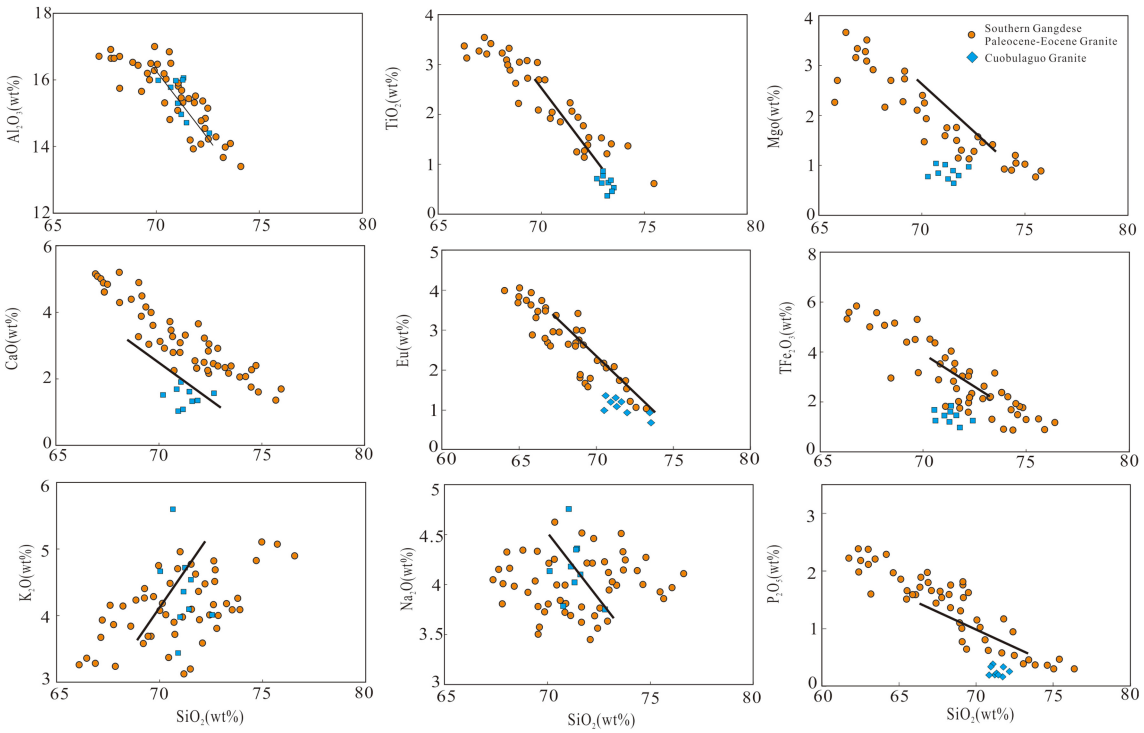

Fig. 6 Harker diagram of the Cuobulaguo granite. Other Eocene granite in the southern Gangdese terrane are from Xu (2010)

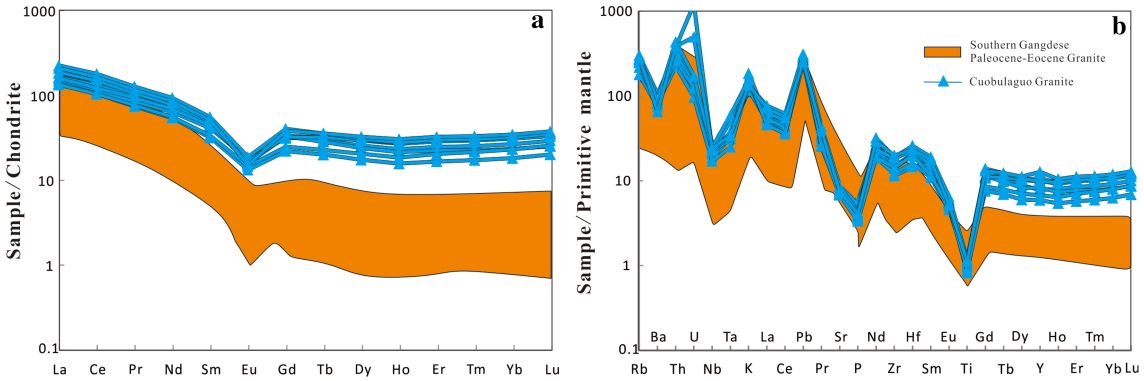

Fig. 7 Chondrites-normalized map of rare earth element patterns (**a**) and primitive mantle-normalized trace elements patterns (**b**) of the Cuobulaguo granite (standardized values according to Sun and Mcdonough 1989). Other Eocene granite in the southern Gangdese terrane are from Xu (2010)

et al. 2006). The Cuobulaguo pluton had high SiO_2 (70.09%–72.64%) and high Na_2O and K_2O (3.86%–4.75%; 3.51%–5.55%). At the same time, it had low P_2O_5 (0.07%–0.12%), low MgO (0.41%–0.76%), and low TiO_2 (0.08%–0.24%). In addition, all samples had moderately-strong Eu negative anomalies (δEu of 0.35 to 0.51), and were enriched in the large ion lithophile elements (LILEs), such as Rb, Th, and K. Among the high-field-strength elements (HFSE), the sample negative Nb, P, Ba, Ti anomalies (Fig. 7b). The granite in our study mainly consists of plagioclase, quartz, and K-feldspar with minor amounts of hornblende and biotite (Fig. 2d, e), but lack muscovite and other Al-rich minerals. The samples have A/CNK < 1.1, but the samoles were hornblende-bearing granite. P had a very low solubility in aluminous or slightly aluminous solutions, which decreases as the degree of differentiation (Pichavant et al. 1992). The P_2O_5 contents decrease with the increase of the SiO_2 contents (Fig. 6), which adjusts to the trend of evolution of the I-type granite; Its characteristics are important criteria for distinguishing I-type granite (Chappell and White 1992). Therefore, this petrological composition is characteristic of I-type granite rather than S-type granite. In addition, our field observations of rock assemblages and the granite's low Cr content of 5.94 to

12.03 ppm indicate that the granite did not form by partial melting of an ophiolite, which also excludes M-type granites. This is also confirmed by plotting our samples in the geochemical discrimination diagrams in Fig. 8, which show that the granite not fractioned and is an I-type granite.

5.2 Granite magma source area and evolution

Previous studies show that partial melting of the crust can produce granites in large quantities (Leake 1990). The formation of I-type granites may have two reasons: (1) The formation of I-type granites results from the partial melting of intermediate-base igneous rocks or metamorphic rocks in the crust (Chappell and Stephens 1988); (2) I-type granite formation by a mantle source during the bark melting process (Kemp et al. 2007). Taking into account the regional context and the petrological characteristics, we conclude that the granite is derived from the partial melting of metamorphic rocks of the Earth's crust.

In general, voluminous granites are usually formed by partial melting of the crust. In geochemistry, the main granitic elements of Cuobulaguo TiO_2, MgO, Al_2O_3, CaO, MnO, K_2O and Na_2O have a good linear relationship with SiO_2 and the granite can undergo a mixture of magma (Fig. 6). The loss of Cuobulaguo granite from Sr, Ba and Eu trace elements reflects the separation and crystallization of plagioclase and K-feldspar during granite formation (Qiu et al. 2005). According to the Fig. 8b (Lai et al. 2007), Separation and crystallization of plagioclase and K-feldspar are mainly found in the diagenesis process of the Cuobulaguo pluton.

In the rare earth partitioning diagram and the microelement cobweb diagram, the granite samples were enriched in LILE of large ions (Rb, Th, U, K and Pb) and the loss of High intensity field elements (HFSE), such as Ba, P, and Ti, which had the geochemical characteristics of crust or arc magmatic rocks (Kelemen et al. 1990). The geochemical characteristics of the samples indicate that the source rocks of the granite are closely related to the lower crust. In addition, the loss of Sr, P, and Ti shows to some extent the geochemical characteristics of the igneous rocks related to subduction, while the loss of Ba and Nb reflects the characteristics of the continental crust of the region of origin. Combinations of trace elements are very useful for discriminating the tectonic adjustment of magma, such as Nb/Ta, Th/Ta, Y/Nb, and La/Nb (Sun and McDonough 1989). The value of the sample in Nb/Ta was between 7.32 and 12.42, a value close to the average value of the crust and much lower than the initial melting value of the mantle and derived from it. The value of Th/Ta is 9.16 to 26.33, which is much higher than the genetic rocks of original mantle, and is relatively close to the mean value of the crust (Th/Ta = 11.67, Rudnick and Gao 2003). Value of Y/Nb (< 1.2), while crust genetic rocks have a value greater than 1.2 (Eby 1992). The Y/Nb value of the samples in the study area is between 1.73 and 3.16, indicating that the samples are the product of the molten differentiation of the source of the crust. In addition, the ratio La/Nb of the sample was between 1.77 and 3.28, with an average value of 2.53, both greater than 1.0, which was different from the mantle. The Zr versus Zr/Sm diagram (Fig. 9a) can be used to judge magmatic genesis and the samples show a positive correlation, indicating that partial melting is the main process of Cuobulaguo granitoid diagenesis. In the Nb versus Nb/Th diagram (Fig. 10a), the samples have the same geochemical properties as the volcanic arcs. In

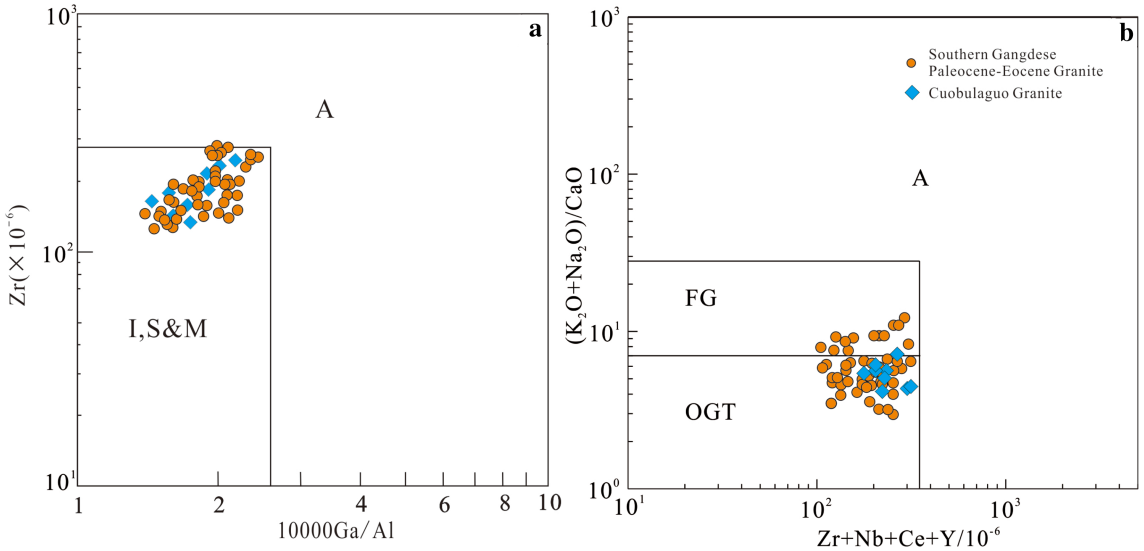

Fig. 8 Zr versus 10000 Ga/Al and $(K_2O + Na_2O)/CaO$ versus Zr + Nb + Ce + Y discriminant diagram of the Cuobulaguo granite (**a**, **b** according to Whalen and Chappell 1998). Other Eocene granite in the southern Gangdese terrane are from Xu (2010)

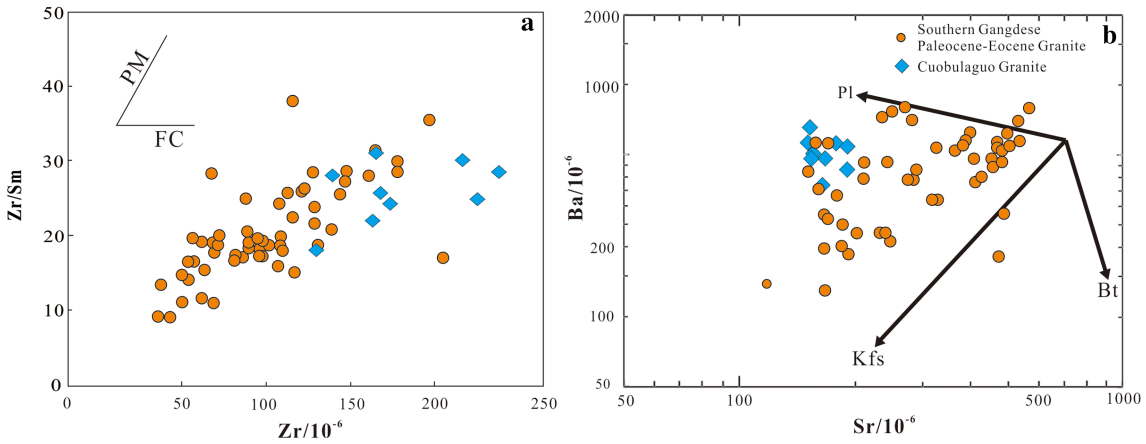

Fig. 9 Schematic diagram of Zr/Sm versus Zr (**a**) and Ba versus Sr of the Cuobulaguo granite (according to Schiano et al. 2010). Other Eocene granite in the southern Gangdese terrane are from Xu (2010)

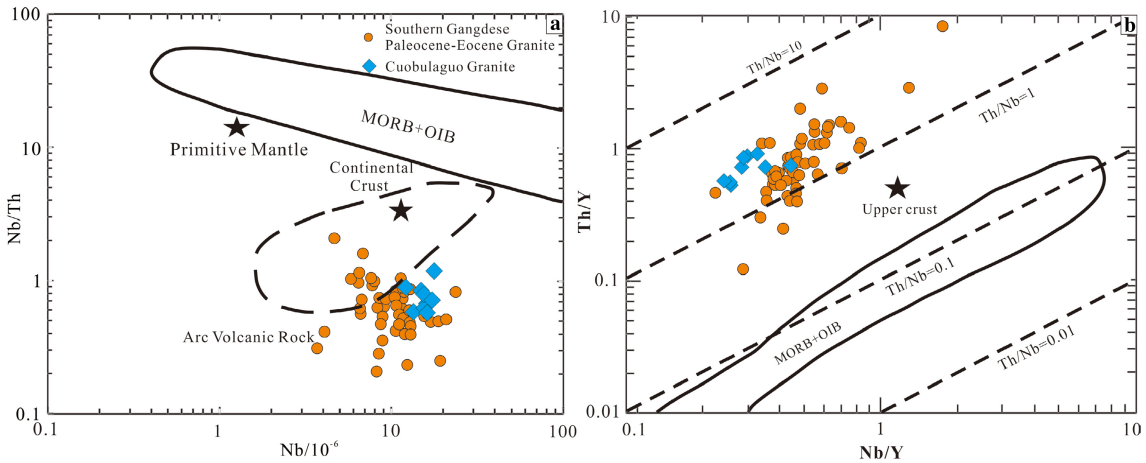

Fig. 10 Nb/Th versus Nb (**a**) and Th/Y versus Nb/Y (**b**) diagrams of the Cuobulaguo granite (according to Boztuğ et al. 2007). Other Eocene granite in the southern Gangdese terrane are from Xu (2010)

the Nb/Y versus Th/Y diagram (Fig. 10b), the samples are located between the Th/Nb = 1 and Th/Nb = 10 trends, close to the average composition of the lower crust. The low MgO and Cr content in the samples also indicated that the granite of the region had been partially melted from the material of the crust source material. In addition, according to the Fig. 9b (Lai et al. 2007), minerals such as plagioclase and apatite have been separated and crystallized during the process of diagenesis granite of Cuobulaguo. This was consistent with the moderately Eu negative anomalies (δEu of 0.35 to 0.51). The granite sample in the study area has fewer $Mg^{\#}$ values (6.7–13.6), which are less than 45, indicating that the main magma does not interact with the mantle.

Experiments in petrology have shown that in a wide range of temperature and pressure conditions, partial melting of the continental crust with different components would produce different types of granite magma (Skjerlie and Patiño Douce 2002). The partial fusion of the sedimentary rocks in the crust usually produces acidic and acidic granites, while the partial fusion of the middle and basic rocks in the crust produces I-type granite basal alumina (Sisson et al. 2005). Nb/Th ratio (1.1–1.3) is similar to the ratio of the source of the crust, significantly lower than the proportion of the mantle source (> 15), suggesting that granite magma not be partially melted from mantle Peridotite or partially melted of basaltic magma. Al_2O_3/(MgO + FeOT) versus CaO/(MgO + FeOT) of the magma are related to the source material of the rock and the ratio can discriminate the source material of the intermediate-acid magma rock. Combined with the discriminant plot of the region of origin of the granite (Fig. 10), Cuobulaguo granite samples fall into the partially melted sandstone of the metamorphic sandstone, indicating that it comes from the partial fusion of the metamorphic sandstone of the crust.

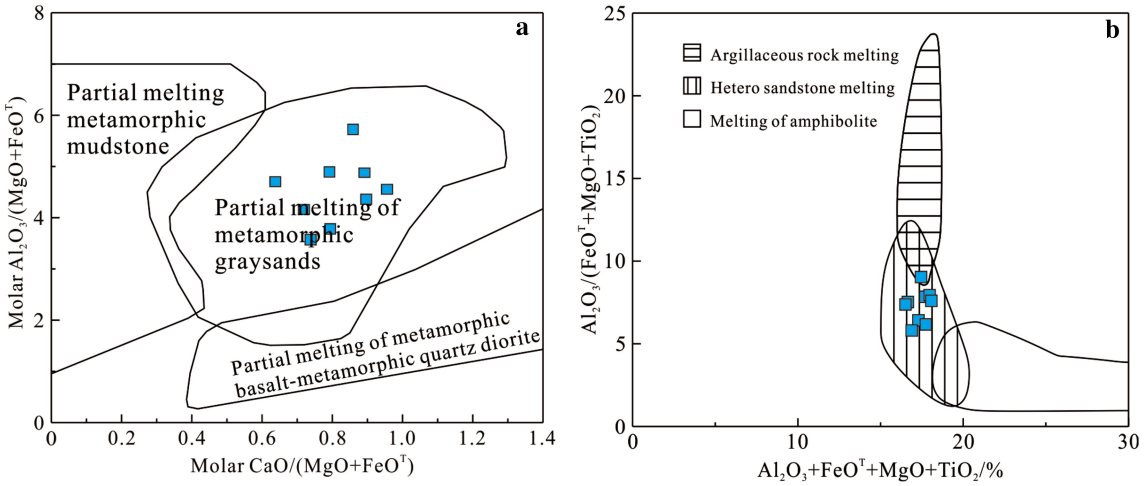

Fig. 11 Distinguishing diagram of the original rock type of the Cuobulaguo granite (**a** according to Altherr et al. 2000) (**b** according to Douce 1999)

In summary, the Cuobulaguo granite formation may come from the lower crust being partially melted and formed (Fig. 11).

5.3 Tectonic background

Igneous rocks are commonly used to reconstruct the tectonic configuration, given the link between magma generation and plate tectonics (Winter 2001). As we all know, southern Gangdese Terrane considered the most magmatic region of the Qinghai-Tibetan plateau. Paleocene-Eocene Gangdese (65–41 Ma) is the peak of magmatic activity. Previous studies have shown that the main body of the Gangdese rock base is granite, mainly affected by the continental collision between India and Asia, the Neo-Tethy oceanic slab detachment and subduction and collision north of the basin. Himalayan-Tethys oceanic on the south side. Rupture of the Neo-Tethy oceanic slab at the beginning of the continental collision between India and Asia. To the south of Gangdese occurred large-scale calc-alkaline volcanic eruptions and subsequent small-scale intrusion, forming Dianzhong formation and the Linzizong formation volcanic rocks, as well as a small amount of intrusive acidic rock (Mo et al. 2005; Xu 2010; Dong 2008). Although much research has been done, there are still differences between the India-Asia continental collision and disappearance of the Neo-Tethys oceanic (Rowley 1998; Yin and Harrison 2000; Aitchison et al. 2007). Lee and Lawver (1995) suggested that the India-Asia continent had a "soft collision" around 65 Ma and that a "hard collision" occurred around 45 Ma; Hou et al. (2006) considered that the India-Asia continental collisions were divided into three stages: main collision (65–41 Ma), late collision (40–26 Ma) and backward collision (25–0 Ma). Mo et al. (2007) suggested that the India-Asia continent collided around 70–65 Ma and the collision ended around 40 Ma, and the Neo-Tethys oceanic disappeared. According to the results of previous statistics (Garzanti et al. 1987; Yin and Harrison 2000; Aitchison et al. 2002, 2007; Mo et al. 2007; Najman et al. 2010; Bouilhol et al. 2013; Donaldson et al. 2013; Hu et al. 2015, 2016; Yang et al. 2015; Zhu et al. 2015; Ding et al. 2016; Meng et al. 2016a, b), most researchers believe that continental collisions information Indian–Asian are from the Late Paleocene to the Early Eocene (60–55 Ma). The Cuobulaguo pluton in this study formed in 61–59 Ma, thereby providing a valuable case study for understanding the Paleocene magmatism, and limit the initial collision time of the India-Asian continental and geodynamics of the southern Gangdese subterrane.

The specific tectonic setting forms a certain type of magmatic rock, and the tectonic setting of the magmatic rock can be judged by its characteristics of geochemical composition (Dong 2008). In the discrimination of the tectonic environment, elements of high field intensity are usually selected as Nb, Y, Ta, and Yb. They have a low ion energy potential, are relatively stable during weathering, alteration, and metamorphism of rocks and, in general, do not migrate. Insensitive to reflection and separation of crystallization and assimilation, it can represent the composition of the region of origin. At the same time, we can also choose trace elements with different activities, for example, Rb/30 versus Hf versus 3Ta and Rb versus Y + Yb (Fig. 12), the samples fall into the granite of the post-collision granite and volcanic arc granite, reflecting the environment of the magma formation after the collision, which may be the orogenic stage or the collision stage, reflecting the environment of Formation of the magma after the collision of Cuobulaguo, suggests that the

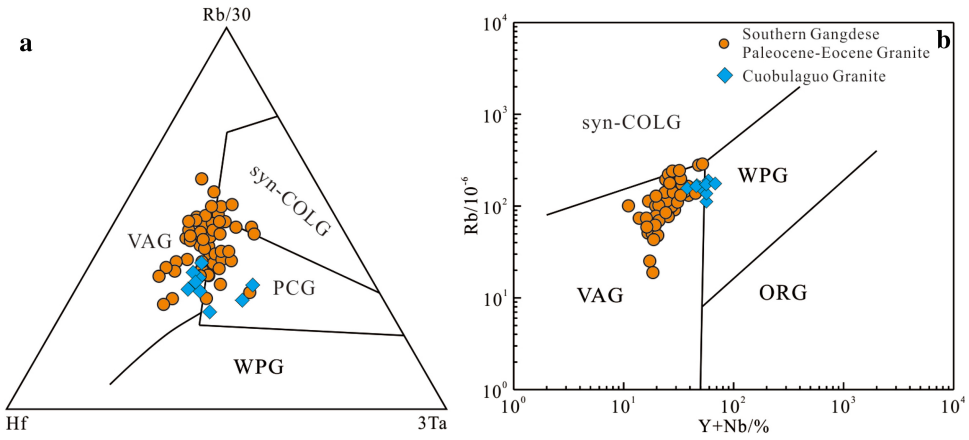

Fig. 12 Discriminant diagram of Rb/30 versus Hf versus 3Ta (**a** according to Pearce et al. 1984) and Rb versus Y + Yb (**b** according to Zhang et al. 2008) tectonic backgrounds of the Cuobulaguo granite. Other Eocene granite in the southern Gangdese terrane are from Xu (2010)

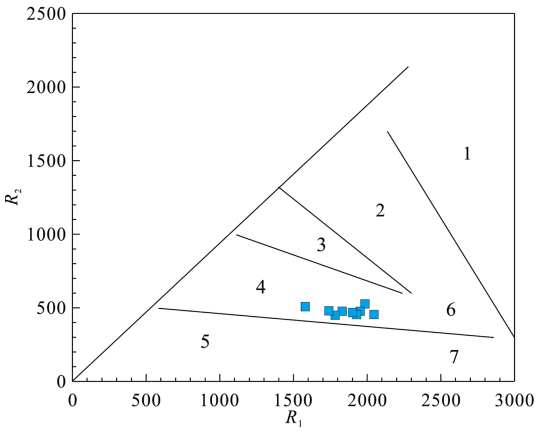

Fig. 13 Discriminant diagram of the structural background of R_2 versus R_1 (according to Batchelor 1985). 1-Mantle plagioclase granite; 2-destructive mobile plate margin (pre-collision) granite; 3-post collision uplift granite; 4-late orogenic granite; 5-anorogenic A-type granite; 6-syn-collision(S-type) granite; 7-post orogenic A-type granite

Indian–Asian continent in the middle of the Paleocene collided.

Combined with the R_2 versus R_1 granite diagram (Fig. 13), all samples are in the late orogenic granite zone, indicating that the formation environment corresponds to the granite after the collision, indicating that it may be formed in the late stage of the collision. Since the post-collision environment is relatively complex, it is not possible to distinguish its tectonic environment solely by chemical illustration. It must be considered in combination with other geological facts. The activity of the magma formed by the tectonic environment after the collision has common characteristics: mainly for high-K calc-alkaline granites, peraluminous and alkaline–alkaline granules on alkali are also more numerous, but are separated from each other; post-collisional magmatism is related to horizontal movement along the shear zone; The area of origin contains a large number of new components, newly formed volcanic rocks or sedimentary rock features.

The Cuobulaguo granites in this study were formed at 61–59 Ma. According to previous research, in the shallow low-pressure source area, the minerals are mainly plagioclase. At that time, a large number of Sr and plagioclase Ca have isomorphism and have low Sr/Y and La/Yb ratio characteristics in the molten state (Moyen 2009); In areas of deep high pressure, minerals are mainly amphiboles and garnets, and their melts have high proportions of Sr/Y and La/Yb (Zhu et al. 2017); The results of the test show that the samples have a lower Sr/Y and La/Yb ratio, suggesting that the granite is formed in a shallow environment at low pressure. According to research carried out by Wang and his collaborators (2017), in the Gangdese Belt of 80–70 Ma, there are magmatic rocks with high proportions of Sr/Y and La/Yb, which indicate that the Gangdese have suffered a process similar uprising in the collision of the Andes of the Asian continent; Magmatic rocks exposed at the base of Gangdese (70–65 Ma) have begun to become rare and do not have the characteristics of a thickened lower crust. The Neo-tethyan oceanic slab can have low angle subduction before 70 Ma, and the 70–65 Ma subduction slab can rebound or be at the beginning of the collision between the Indian and Asian continents (Tian et al. 2016; Li et al. 2016).

After the initial continental collision between Indian and Asia, the continuous subduction of the dense Neo-Tethyan oceanic slab generated a great downward force in the floating continental lithosphere that is resistant to subduction the continued subduction (Davies and von Blanckenburg 1995). This situation of opposing forces created a strong deformation of the extension in the slab, which resulted in a narrow zone of break off and finally the detachment of the Neo-Tethyan oceanic slab at ~ 61 Ma. Granite production containing muscovite often marks the conversion of the tectonic environment (Hou et al. 2006). The roll-back of the slab usually takes place at the end of the oceanic subduction and at the beginning of the collision between the Earth and the continent and gives way to the

burial in depth of the continental slab (Brun and Faccenna 2008). Consequently, at 61 Ma, the Neo-Tethys oceanic slab suffered a roll-back of the slab, causing upwelling of mantle material. Provide a sufficient source of heat for the material of the lower crust, melting the lower crust to form an early granite.

Based on the previous analysis, the tectonic framework formed by the Cuobulaguo granite may be the post-collision crust extension stage and belongs to the post-collision environment. This paper estimates that the initial moment of the continental collision between India and Asia is no later than 61 Ma. With the onset of the continental collision between India and Asia, the Neo-Tethys oceanic slab subduced by subduction is separated from the continental plate by gravity, causing the upwelling of the asthenosphere, thereby inducing partial melting of the lithospheric mantle to produce intermediate-acid magma. And bottoming into the bottom of the lower crust, and then inducing partial melting of the lower crust to form Cuobulaguo granitic.

6 Conclusion

1. The U–Pb ages of the zircon LA-ICP-MS in the Cuobulaguo granites are $61.3 \pm 1.4 \sim 59.5 \pm 1.1$ Ma, indicating formation during the Middle Paleocene.
2. The Cuobulaguo granite belongs to I-type granite. The granite samples were enriched in LILE of large ions (Rb, Th, U, K, and Pb) and the loss of High-intensity field elements (HFSE), such as Ba, P and Ti. It has geochemical characteristics of crust or arc magmatic rocks.
3. The collision of the Indian–Asia continent and break off of the Neo-Tethys oceanic slab was responsible for the generation of the Cuobulaguo granite and, more generally, for the Paleocene magmatism in the southern Gangdese subterrane.

Acknowledgements The fieldwork was guided by Professor. Zhu Lidong and Dr. Yang Wenguang. They participated in the fieldwork, which werehelped by Yang Zhen, Lu Zhiyou, Su Xin, Li Limin, Zhang Hongliang, Mai Yuanjun, and Hu Juncheng at University of Chinese Academy of Sciences. Valuable comments from reviewers on this article are appreciated.

References

Aitchison JC, Davis AM, Badengzhu Lou H (2002) New constraints on the India-Asia collision: the lower Miocene Gangrinboche conglomerates, Yarlung Tsangpo suture zone, SE Tibet. J Asian Earth Sci 21(3):251–263

Aitchison JC, Ali JR, Davis AM (2007) When and where did India and Asia collide? J Geophys Res Solid Earth 112(B5):B05423

Allègre CJ, Rousseau D (1984) The growth of the continent through geological time studied by Nd isotope analysis of shales. Earth Planet Sci Lett 67(1):19–34

Altherr R, Holl A, Hegner E, Langer C, Kreuzer H (2000) High-potassium, calc-alkaline I-type plutonism in the European Variscides: northern Vosges (France) and northern Schwarzwald (Germany). Lithos 50(1):51–73

Batchelor RA (1985) Petrogenetic interpretation of granitoid rock series using multicationic parameters. Chem Geol 48(1):43–55

Bonin B (2007) A-type granites and related rocks: evolution of a concept, problems and prospects. Lithos 97(1–2):1–29

Bouilhol P, Jagoutz O, Hanchar JM, Dudas FO (2013) Dating the India-Eurasia collision through arc magmatic records. Earth Planet Sci Lett 366(2):163–175

Boztuğ D, Harlavan Y, Arehart GB, Satir M, Avci N (2007) K–Ar age, whole-rock and isotope geochemistry of A-type granitoids in the Divriği-Sivas region, eastern-central Anatolia, Turkey. Lithos 97(1–2):193–218

Brun JP, Faccenna C (2008) Exhumation of high-pressure rocks driven by slab rollback. Earth Planet Sci Lett 272(1–2):1–7

Chappell BW (1999) Aluminium saturation in I- and S-type granites and the characterization of fractionated haplogranites. Lithos 46(3):535–551

Chappell BW, White JR (1974) Two contrasting granite type. Pac Geol 8:173–174

Chappell BW, Stephens WE (1988) Origin of infracrustal (I-type) granite magmas. Trans Royal Soc Edinb Earth Sci 79(2–3):71–86

Chappell BW, White AJR (1992) I- and S-type granites in the Lachlan Fold Belt. Trans Royal Soc Edinb Earth Sci 83(1–2):1–26

Chu MF, Chung SL, Song B, Liu D, O'Relly SY, Pearson NJ, Ji JQ, Wen DR (2006) Zircon U-Pb and Hf isotope constraints on the Mesozoic tectonics and crustal evolution of southern Tibet. Geology 34(9):745–748

Chu MF, Chung SL, O'Reilly SY, Pearson NJ, Wu FY, Li XH, Liu DY, Ji JQ, Chu CH, Lee HY (2011) India's hidden inputs to Tibetan orogeny revealed by Hf isotopes of Transhimalayan zircons and host rocks. Earth Planet Sci Lett 307(3):479–486

Chung SL, Liu DY, Ji JQ, Chu MF, Lee HY, Wen DJ, Lo CH, LeeTY Qian Q, Zhang Q (2003) Adakites from continental collision zones: melting of thickened lower crust beneath southern Tibet. Geology 31(11):1021–1024

Chung SL, Chu MF, Zhang YQ, Xie YW, Lo CH, Lee TY, Lan CY, Li XH, Zhang Q, Wang YZ (2005) Tibetan tectonic evolution inferred from spatial and temporal variations in post-collisional magmatism. Earth-Sci Rev 68(3):173–196

Chung SL, Chu MF, Ji J, O'Relly SY, Pearson NJ, Liu DY, Lee TY, Lo CH (2009) The nature and timing of crustal thickening in Southern Tibet: geochemical and zircon Hf isotopic constraints from postcollisional adakites. Tectonophysics 477(1):36–48

Davies JH, von Blanckenburg F (1995) Slab breakoff: amodel of lithosphere detachment and its test in themagmatismand deformation of collisional orogens. Earth Planet Sci Lett 129:85–102

Ding HX, Zhang ZM, Dong X, Tian ZL, Xiang H, Mu HC, Gou ZB, Shui XF, Li WC, Mao LJ (2016) Early Eocene (ca. 50 Ma) collision of the Indian and Asian continents: constraints from the North Himalayan metamorphic rocks, southeastern Tibet. Earth Planet Sci Lett 435:64–73

Donaldson DG, Webb AAG, Menold CA, Kvlander-Clark ARC, Hacker BR (2013) Petrochronology of Himalayan ultrahigh-pressure eclogite. Geology 41(8):835–838

Dong X (2008) Geochronology and geochemistry of the Mesozoic and Cenozoic granites in the southwestern part of the Gangdese belt, Tibet. Master dissertation, China University of Geosciences (Beijing) **(in Chinese with English abstract)**

Dong GC, Mo XX, Zhao ZD, Guo TY, Wang LL, Chen T (2005) Geochronologic constraints on the magmatic underplating of the Gangdise belt in the India-Eurasia collision: evidence of SHRIMP II zircon U–Pb dating. Acta Geol Sin 79(6):787–794

Dong GC, Mo XX, Zhao ZD, Zhu DC, Song YT, Wang L (2008) Gabbros from southern Gangdese: implication for mass exchange between mantle and crust. Acta Petrol Sin 24(2):203–210 **(in Chinese with English abstract)**

Douce PAE (1999) What do experiments tell us about the relative contributions of crust and mantle to the origin of granitic magmas? Underst Granites Integr New Class Tech 168(1):55–75

Eby GN (1992) Chemical subdivision of A-type granitoids: petrogenesis and tectonic implications. Geology 20(7):641

Garzanti E, Baud A, Mascle G (1987) Sedimentary record of the northward flight of India and its collision with Eurasia (Ladakh Himalaya, India). Geodin Acta 1(4–5):297–312

He ZH, Yang DM, Zheng CQ, Huang YC (2005) Geochemical characteristics and tectonic significance of Indosinian granites in the Menba area of Gangdese, Tibet, China. Chin J Geol 24(4):354–359 **(in Chinese with English abstract)**

Hou ZQ, Mo XX, Yang ZM, Wang AJ, Pan GT, Qu XF, Nie FJ (2006) Metallogeneses in the collisional orogen of the Qinghai-Tibet Plateau: tectonic setting, tempo-spatial distribution and ore deposit types. Chin J Geol 33(2):340–351 (**in Chinese with English abstract**)

Hou ZQ, Wang EQ, Mo XX, Ding L, Pan GT, Zhang ZJ (2008) Collisional orogeny and metallogenesis of the Tibetan Plateau. Geological Publishing House, Beijing, pp 1–980 **(in Chinese)**

Hu XM, Garzanti E, Moore T, Taffi I (2015) Direct stratigraphic dating of India-Asia collision onset at the Selandian (middle Paleocene, 59 ± 1 Ma). Geology 43(10):859–862

Hu XM, Garzanti E, Wang JG, Huang WT (2016) The timing of India-Asia collision onset: facts, theories, controversies. Earth Sci Rev 160:264–299

Ji WQ, Wu FY, Chung SL, Li JX, Liu CZ (2009a) Zircon U-Pb geochronology and Hf isotopic constraints on petrogenesis of the Gangdese batholith, southern Tibet. Chem Geol 262(3):229–245

Ji WQ, Wu FY, Liu CZ, Chung SL (2009b) Geochronology and petrogenesis of granitic rocks in Gangdese batholith, southern Tibet. Sci China 52(9):1240–1261

Ji WQ, Wu FY, Zhai SL, Liu CZ (2009c) Age and rock genesis of the Gangdese rock-based granite in southern Tibet. Sci China Earth Sci 39(7):849 **(in Chinese with English abstract)**

Ji WQ, Wu FY, Liu CZ, Chung SL (2012) Early Eocene crustal thickening in southern Tibet: new age and geochemical constraints from the Gangdese batholith. J Asian Earth Sci 53(2):82–95

Ji WQ, Wu FY, Chung SL, Wang XC, Liu CZ, Li QL, Liu ZC, Liu XC, Wang JG (2016) Eocene Neo-Tethyan slab breakoff constrained by 45 Ma oceanic island basalt-type magmatism in southern Tibet. Geology 44(4):283–286

Kelemen PB, Johnson KTM, Kinzler RJ, Irving AJ (1990) High-field-strength element depletions in arc basalts due to mantle–magma interaction. Nature 345(6275):521–524

Kemp AIS, Hawkesworth CJ, Foster GL, et al (2007) Magmatic and crustal differentiation history of granitic rocks from Hf-O isotopes in Zircon. Science 315(5814):980–983

Lai SC, Qin JF, Li YF, Long P (2007) Geochemistry and Sr-Nd-Pb isotopic characteristics of the Mugouriwang Cenozoic volcanic rocks from Tibetan Plateau: constraints on mantle source of the underplated basic magma. Sci China 50(7):984–994

Leake BE (1990) Granite magmas: their sources, initiation and consequences of emplacement. J Geol Soc 147(4):579–589

Lee TY, Lawver LA (1995) Cenozoic plate reconstruction of Southeast Asia. Tectonophysics 251(1–4):85–138

Li XW, Mo XX, Scheltens M, Guan Q (2016) Mineral chemistry and crystallization conditions of the Late Cretaceous Mamba pluton from the eastern Gangdese, Southern Tibetan Plateau. J Earth Sci 27(4):545–570

Liu Y, Liu HC (1996) Quantitative determination of more than 40 trace elements in rock samples by ICP-MS. Geochemistry 6:552–558 **(in Chinese with English abstract)**

Liu YS, Hu ZC, Zong KQ, Gao CG, Gao S, Juan Xu, Chen HH (2010) Reappraisement and refinement of zircon U-Pb isotope and trace element analyses by LA-ICP-MS. Sci Bull 55(15):1535–1546

Ludwig KR (2003) ISOPLOT 3.0: a geochronological toolkit for Microsoft Excel. Berkeley Geochronol Cent 192:59–79

Ma XX, Meert JG, Xu ZQ, Zhao ZB (2017) Evidence of magma mixing identified in the Early Eocene Caina pluton from the Gangdese Batholith, southern Tibet. Lithos 278–281:126–139

Meng YK, Xu ZQ, Santosh M, Ma XX, Chen XJ, Guo GL, Liu F (2016a) Late Triassic crustal growth in southern Tibet: evidence from the Gangdese magmatic belt. Gondwana Res 37:449–464

Meng YK, Dong HW, Cong Y, Xu ZQ, Gao H (2016b) The early-stage evolution of the Neo-Tethys ocean: evidence from granitoids in the middle Gangdese batholith, southern Tibet. J Geodyn 94-95:34–49

Meng YK, Xu ZQ, Gao CS, Xu Y, Li RH (2018) Determination of the Eoceneic magmatism in the middle section of the Gangdese belt, southern Tibet, and its tectonic significance. Acta Petrol Sin 34(3):513–546 **(in Chinese with English abstract)**

Middlemost EAK (1994) Naming materials in the magma/igneous rock system. Annu Rev Earth Planet Sci 37(3–4):215–224

Mo XX, Zhao ZD, Deng JF, Dong GC, Zhou S, Guo TY, Zhang SQ, Wang LL (2003) Response of volcanism to the India-Asian collision. Earth Sci Front 10(3):136–149 **(in Chinese with English abstract)**

Mo XX, Dong GC, Zhao ZD, Zhou S, Wang LL, Qiu RZ, Zhang FQ (2005) Spatial and temporal distribution and characteristics of granitoids in the Gangdese, Tibet and implication for crustal growth and evolution. Geol J China Univ 11(3):281–290 **(in Chinese with English abstract)**

Mo XX, Hou Z, Niu Y, Dong GC, Qu XM, Zhao ZD, Yang ZM (2007) Mantle contributions to crustal thickening during continental collision: evidence from Cenozoic igneous rocks in southern Tibet. Lithos 96(1):225–242

Mo XX, Niu YL, Dong GC, Zhao ZD, Hou ZQ, Zhou S, Ke S (2008) Contribution of syncollisional felsic magmatism to continental crust growth: a case study of the Paleogene Linzizong volcanic Succession in southern Tibet. Chem Geol 250(1):49–67

Mo XX, Zhao ZD, Yu XH, Dong GC, Li YG, Zhou S, Liao ZL, Zhu DC (2009a) Cenozoic collisional-postcollisional igneous rocks in the Tibetan Plateau. Geological Publishing House, Beijing, pp 1–396 **(in Chinese)**

Mo XX, Dong GC, Zhao ZD, Zhu DC, Zhou S (2009b) Mantle input to the crust in Southern Gangdese, Tibet, during the Cenozoic: zircon Hf isotopic evidence. J Earth Sci 20(2):241–249

Moyen JF (2009) High Sr/Y and La/Yb ratios: The meaning of the "adakitic signature". Lithos 112(3):556–574

Najman Y, Appel E, Boudagher-Fadel M, Bown P, Carter A, Garzanti E, Godin L, Han JT, Liebke U, Oliver G, Parrish R, Vezzoli G (2010) Timing of India-Asia collision: geological, biostratigraphic, and palaeomagnetic constraints. J Geophys Res 115(B12):1–70

Pan GT, Mo XX, Hou ZQ, Zhu DC, Wang LQ, Li GM, Zhao ZD, Geng QR, Liao ZL (2006) Spatial-temporal framework of the

Gangdese orogenic belt and its evolution. Acta Petrol Sin 22(3):521–533 **(in Chinese with English abstract)**

Pearce JA, Harris NBW, Tindle AG (1984) Trace element discrimination diagrams for the tectonic interpretation of granitic rocks. J Petrol 25(4):956–983

Peccerillo A (1976) Geochemistry of eocene calc-alkaline volcanic rocks from the Kastamonu area, Northern Turkey. Contrib Mineral Petrol 58(1):63–81

Pichavant M, Montel JM, Richard LR (1992) Apatite solubility in peraluminous liquids: experimental data and an extension of the Harrison-Watson model. Geochim Cosmochim Acta 56(56):3855–3861

Qiu JS, Hu J, Wang XL, Jiang SY, Wang RC, Xu XS (2005) The Baishigang Pluton in Heyuan, Guangdong Province: a highly fractionated I-type granite. Chin J Geol 79(4):503–514 (**in Chinese with English abstract**)

Rickwood PC (1989) Boundary lines within petrologic diagrams which use oxides of major and minor elements. Lithos 22(4):247–263

Rowley DB (1998) Minimum age of initiation of collision between India and Asia North of Everest based on the subsidence history of the Zhepure Mountain section. J Geol 106(2):220–235

Rudnick RL, Gao S (2003) Composition of the continental crust. Treatise Geochem 3:1–64

Schiano P, Monzier M, Eissen JP, Martin H, Koga KT (2010) Simple mixing as the major control of the evolution of volcanic suites in the Ecuadorian Andes. Contrib Miner Petrol 160(2):297–312

Searle MP, Windley BF, Coward MP, Cooper DJW, Rex AJ, Rex D, Li TD, Xiao XC, Jan MQ, Thakur V, Kumar S (1987) The closing of Tethys and the tectonics of the Himalaya. Geol Soc Am Bull 98(6):678–701

Sisson TW, Ratajeski K, Hankins WB, Glazner AF (2005) Voluminous granitic magmas from common basaltic sources. Contrib Miner Petrol 148(6):635–661

Skjerlie KP, Patiño Douce AE (2002) The fluid-absent partial melting of a zoisite-bearing quartz eclogite from 1.0 to 3.2 GPa; implications for melting in thickened continental crust and for subduction-zone processes. J Petrol 43(2):291–314

Sun SS, Mcdonough WF (1989) Chemical and isotopic systematics of oceanic basalts: implications for mantle composition and processes. Geol Soc Lond Spec Publ 42(1):313–345

Sun X, Zheng YY, Xu J, Huang LH, Guo F, Gao SB (2017) Metallogenesis and ore controls of Cenozoic porphyry Mo deposits in the Gangdese belt of Southern Tibet. Ore Geol Rev 81:996–1014

Tang JX, Lang XH, Xie FW, Gao YM, Li ZJ, Huang Y, Ding F, Yang HH, Zhang L, Wang Q, Zhou Y (2015) Geological characteristics and genesis of the Jurassic No.1 porphyry Cu-Au deposit in the Xiongcun district, Gangdese porphyry copper belt, Tibte. Ore Geol Rev 70:438–456

Tian YT, Kohn BP, Phillips D, Hu SB, Gleadow AJW, Carter A (2016) Late Cretaceous-earliest Paleogene deformation in the Longmen Shan fold-and-thrust belt, eastern Tibetan Plateau margin: pre-Cenozoic thickened crust? Tectonics 35(10):2293–2312

Wang Q (2016) Origin and petrogenesis of the post-collisional magmatism in both north and south sides of Lhasa terrane. Doctoral dissertation, China University of Geosciences (Beijing), pp 1–123 **(in Chinese with English abstract)**

Wang EC (2017) Timing of the initial collision between the Indian and Asian continents. Sci China Earth Sci 60(4):626–634

Wang R, Richards JP, Hou ZQ, An F, Creaser RA (2015) Zircon U-Pb age and Sr–Nd–Hf–O isotope geochemistry of the Paleocene-Eocene igneous rocks in western Gangdese: evidence for the timing of Neo-Tethyan slab breakoff. Lithos 224–225:179–194

Wang ZZ, Liu D, Zhao ZD, Yan JJ, Shi QS, Mo XX (2017) The Sangri highly fractionated I-type granites in southern Gangdese: petrogenesis and dynamic implication. Acta Petrol Sin 33(8):2479–2493 (**in Chinese with English abstract**)

Wen DR, Liu DY, Chung SL, Chu MF, Ji JQ, Zhang Q, Song B, Lee TY, Yeh MW, Lo CH (2008a) Zircon SHRIMP U-Pb ages of the Gangdese Batholith and implications for Neotethyan subduction in southern Tibet. Chem Geol 252(3–4):191–201

Wen DR, Chung SL, Song B, Lizuka Y, Yang HJ, Ji JQ, Liu DY, Gallet S (2008b) Late Cretaceous Gangdese intrusions of adakitic geochemical characteristics, SE Tibet: petrogenesis and tectonic implications. Lithos 105(1):1–11

Whalen JB, Chappell BW (1988) Opaque mineralogy and mafic mineral chemistry of I and S-type granites of the Lachlan fold belt, southeast Australia. Am Minerol 73(3–4):281–296

Winter JD (2001) An introduction to igneous and metamorphic petrology. Prentice Hall, New Jersey, p 697

Xu WC (2010) Spatial variation of zircon U-Pb age and Hf isotopic composition of the Gangdese granitoids in Tibet and its geologic implications. Doctoral dissertation, China University of Geosciences, pp 1–96 **(in Chinese with English abstract)**

Xu ZQ, Yang JS, Li HB, Ji SC, Zhang ZM, Liu Y (2011) On the tectonics of the India-Asia collision. Acta Geol Sin 85(1):1–33 **(in Chinese with English abstract)**

Yang TS, Ma YM, Bian WW, Jin JJ, Zhang SH, Wu HC, Li HY, Yang ZY, Ding JK (2015) Paleomagnetic results from the Early Cretaceous Lakang Formation lavas: constraints on the paleolatitude of the Tethyan Himalaya and the India-Asia collision. Earth Planet Sci Lett 428:120–133

Yin A, Harrison TM (2000) Geologic evolution of the Himalayan-Tibetan Orogen. Annu Rev Earth Planet Sci 28(28):211–280

Zhang Q, Wang YL, Jin WJ, Jia XQ, Li CD (2008) Criteria for the recognition of pre-, syn- and post-orogenic granitic rocks. Geol Bull China 27(1):1–18 **(in Chinese with English abstract)**

Zhang LX, Wang Q, Zhu DC, Jia LL, Wu XY, Liu SA, Hu ZC, Zhao PT (2013a) Hf isotope mapping of zircons in Lhasa terrane: constraints on crustal properties and metallogenic potential. Acta Petrol Sin 29(11):3681–3688 **(in Chinese with English abstract)**

Zhang ZM, Dong X, Xiang H, Liou JG, Santosh M (2013b) Building of the Deep Gangdese Arc, South Tibet: Paleocene Plutonism and Granulite-Facies Metamorphism. J Petrol 54(12):2547–2580

Zhang ZM, Ding L, Zhao ZD, Santosh M (2017) Tectonic evolution and dynamics of the Tibetan Plateau. Gondwana Res 41:1–8

Zhu DC, Pan GT, Mo XX, Wang LQ, Liao ZL, Zhao ZD, Dong GC, Zhou CY (2006) Late Jurassic-Early Cretaceous geodynamic environment in the north-central Gangdese: volcanic rock constraints. Acta Petrol Sin 22(3):534–546 **(in Chinese with English abstract)**

Zhu DC, Pan GT, Chung SL, Liao ZL, Wang LQ, Li GM (2008) SHRIMP zircon age and geochemical constraints on the origin of lower jurassic volcanic rocks from the Yeba Formation, Southern Gangdese, South Tibet. Int Geol Rev 50(5):442–471

Zhu DC, Mo XX, Niu Y, Zhao ZD, Wang LQ, Liu YS, Wu FY (2009) Geochemical investigation of early cretaceous igneous rocks along an east–west traverse throughout the central Lhasa terrane, Tibet. Chem Geol 268(3–4):298–312

Zhu DC, Zhao ZD, Niu YL, Mo XX, Chung SL, Hou ZQ, Wang LQ, Wu FY (2011) The Lhasa Terrane: record of a microcontinent and its histories of drift and growth. Earth Planet Sci Lett 301(1–2):241–255

Zhu DC, Wang Q, Zhao ZD, Chung SL, Cawood PA, Niu YL, Liu SA, Wu FY, Mo XX (2015) Magmatic record of India-Asia collision. Sci Rep 5:14289. https://doi.org/10.1038/srep14289

Zhu DC, Wang Q, Cawood PA, Zhao ZD, Mo XX (2017) Raising the Gangdese Mountains in southern Tibet. J Geophys Res Solid Earth 122(1):214–233. https://doi.org/10.1002/2016JB013508